

Chapter 3

Optical properties of ferrocholesterics

3.1 Introduction

Liquid crystals being made up of anisotropic molecules respond to an external magnetic field due to their diamagnetic anisotropy. This diamagnetic anisotropy of liquid crystals is quite small ($\approx 10^{-7}$ cgs units). Thus one needs high magnetic fields (≈ 1 kGauss) to get any observable effect [1]. The magnetic effects can be enhanced by doping these liquid crystals with small amount of magnetic grains. Many binary systems have been prepared by doping liquid crystal materials with magnetic grains of appropriate size [2,3,4,5]. A nematic and a cholesteric liquid crystalline phases having small elongated magnetic particles suspended uniformly with their magnetization aligned are known as ferronematic and ferrocholesteric phases respectively. Recently even magnetically doped ferrosmeectics and ferrohexagonal lyotropic phases have been prepared [6,7]. The concentration of the suspended particles is so low that there is hardly any interaction between the grains. The mechanical coupling between the grains and the liquid crystal molecules is strong enough to give a stable phase. Generally the size of the grains is about 100 \AA with an aspect ratio of about $10 : 1$. Brochard and de Gennes [8] were the first to study theoretically the structure of ferronematics and ferrocholesteric phases in the presence of magnetic field. Since then there has been a lot of studies on different properties of these systems [9,10,11].

Light propagation in ferrocholesterics becomes meaningful when the magnetic grains are transparent like garnets. Sunil Kumar and Ranganath have studied optics of such a system [12]. However, the effect of inherent Faraday rotation of the grains on the light propagation in these structures has not been considered so far. The direction of magnetization of the grains, whether parallel or perpendicular to the long axis of the grains, is important and leads to different optical properties. There are systems with grains having magnetization parallel to the local director [2] and there are also systems with magnetization perpendicular to the local director [3]. In the former case we get a ferrocholesteric with magnetization gradually twisting with the local director much like a helimagnetic system and in the latter case we will have the magnetization of the grains parallel to the twist axis.

The Faraday rotatory power in the transparent magnetic grains depends on the direction of propagation of light with respect to the magnetization \vec{m} and is given by

$$\rho = V |\vec{m}| \cos \theta_m = \rho_o \cos \theta_m \quad (3.1)$$

Where V is a constant and θ_m is the angle between \vec{m} and the direction of light propagation. This dependence of the Faraday rotation on θ_m leads to optical properties which are very different from those of normal cholesterics. In this chapter we have worked out the optical properties of a ferrocholesteric for light propagation in both Bragg and phase grating modes and tried to bring out salient differences between ferrocholesterics and normal cholesterics.

3.2 Light propagation on the short wavelength side of the Bragg band

Here we consider light propagation parallel to the twist axis for wavelengths much smaller than the pitch of the ferrocholesteric medium. At these wavelengths, the multiple reflections and interference effects inside the ferrocholesteric medium are negligible and can be ignored. Under such conditions, Jones matrix method [14] can be employed to study light propagation through the medium. In this method the medium is regarded as being composed of a large number of infinitesimal thin sections, each section representing an optical element. For example, the cholesteric medium can be considered as made up of piles of linear birefringent plates with the principal axis of successive plate being rotated by a constant angle. The advantage of the Jones method is that the problems can be solved analytically in the present case.

In the case of cholesterics, there are two interesting situations even when $\lambda \ll P$ [15]. Let Υ be half the phase retardation of a single plate and Ω be the twist between successive plates. Then in the limit $\Omega \gg \Upsilon$ the cholesteric medium, to a good approximation, acts as a pure rotator, i.e., the eigenmodes inside the medium are nearly right and left circular states traveling with different velocities so that there will be a rotation in the plane of polarization of the incident linear polarized light. This is known as the de Vries limit. On the other hand in the limit $\Omega \ll \Upsilon$ the incident vibration splits into two linear orthogonal vibrations polarized along the two local principal axes. As these vibrations travel inside the medium they also rotate following the local principal axes. This solution is known as Mauguin's limit.

Sometime this limit is also referred as the adiabatic approximation. This optical property is the main principle behind the working of a twisted nematic cell used for display applications.

Just as a cholesteric even a ferrocholesteric can be considered as made up of piles of linearly birefringent plates having Faraday rotation. The principal axis of the successive plates rotates uniformly along the twist axis. In the discussion below we assume that the magnetic grains are parallel to the local director but with \vec{m} along the twist axis.

3.2.1 Theory

We assume the medium to be twisting along the Z axis. Then for such a uniformly twisted medium the Jones transfer matrix M for the entire sample can be written as [16].

$$\mathbf{M} = \mathbf{S}(q_0 z) \exp[(\mathbf{N}_0 - q_0 \mathbf{S}(\pi/2)) z]. \quad (3.2)$$

where the matrix \mathbf{N}_0 is given by

$$\mathbf{N}_0 = \begin{bmatrix} ik + ig_0 & -ik - \rho \\ \rho & -ik - ig_0 \end{bmatrix} \quad (3.3)$$

Here $2g_0$ is the phase retardation per unit thickness, k is the wavevector in the medium, ρ is the Faraday rotatory power, $q_0 = 2\pi/P$ and S is a rotation matrix that is given by

$$\mathbf{S}(\alpha) = \begin{bmatrix} \cos(\alpha) & -\sin(\alpha) \\ \sin(\alpha) & \cos(\alpha) \end{bmatrix}$$

Substituting for \mathbf{N}_o and S in the equation (3.2) we get

$$\mathbf{M} = \exp(-\imath kz) \mathbf{S}(q_o z) \begin{bmatrix} \cos(\Gamma z) + \imath g_o \frac{\sin(\Gamma z)}{\Gamma} & -(\rho - k) \frac{\sinh(\Gamma z)}{\Gamma} \\ (\rho - k) \frac{\sin(\Gamma z)}{\Gamma} & \cos(\Gamma z) - \imath g_o \frac{\sin(\Gamma z)}{\Gamma} \end{bmatrix} \quad (3.4)$$

Here $\Gamma = \sqrt{g_o^2 + (\rho - k)^2}$. If the electric vector of the incident light is

$$\mathbf{E} = \begin{bmatrix} E_x \\ E_y \end{bmatrix} \quad (3.5)$$

then the emergent electric vector is given by

$$\mathbf{E}' = \begin{bmatrix} E'_x \\ E'_y \end{bmatrix} = \mathbf{M} \begin{bmatrix} E_x \\ E_y \end{bmatrix} = \mathbf{M} \mathbf{E} \quad (3.6)$$

3.2.2 Results

For a general case the \mathbf{M} matrix has a complex structure. But here we discuss the two cases where the matrix has a simple form

Case 1

$|\rho - q_o| \gg |g_o|$ with p and q of opposite signs (i.e. when the direction of propagation of light is opposite to that of \vec{m}). Then

$$\mathbf{M} = \exp(-\imath kz) \begin{bmatrix} \cos(\rho z) & -\sin(\rho z) \\ \sin(\rho z) & \cos(\rho z) \end{bmatrix}$$

The medium, to a good approximation, acts as a pure rotator, i.e. , the solution goes over to de Vries limit. It is interesting to note that the condition $|\rho - q_o| \gg |g_o|$

need not imply that $|q_o| \gg |g_o|$. Here this condition can also be satisfied for small values of q_o , i.e., for large values of pitch. Thus the existence of Faraday rotation can lead to a de Vries limit even for a ferrocholesteric medium of large pitch. This is contrary to the case of the cholesterics where the de Vries limit is obtained only for very small pitch.

Case 2

$|p - q_o| \ll |g_o|$ with p and q of the same sign (when the propagation of light is in the same direction as that of \vec{m}). Then

$$\mathbf{M} = \exp(-ikz) \begin{bmatrix} \cos(q_o z) & -\sin(q_o z) \\ \sin(q_o z) & \cos(q_o z) \end{bmatrix} \begin{bmatrix} \exp(\imath g_o z) & 0 \\ 0 & \exp(-\imath g_o z) \end{bmatrix}$$

This is the Mauguin's solution as in the case of twisted nematic. For non zero ρ the condition $|p - q_o| \ll |g_o|$ can be satisfied even with $|q_o| > |g_o|$. In this situation, in the absence of the Faraday rotation, the solution will go over to the de Vries limit and not to the Mauguin limit.

The two cases discussed above show that depending on the propagation of light along or opposite to the direction of \vec{m} the medium can act as a Mauguin retarder or a de Vries rotator, respectively. For example, this happens for a ferrocholesteric of pitch $\simeq 30\mu\text{m}$, $\rho_o \simeq 2.0 \times 10^3 \text{ rad cm}^{-1}$ and birefringence $\Delta n \simeq 0.0025$. Such a medium between two appropriately aligned polaroids can act as an optical diode, i.e. transmitting light in one direction and blocking it completely in the opposite direction.

3.3 Light propagation in the phase grating mode

Earlier we mentioned that cholesterics and Sc* exhibit optical diffraction [17,18] in the phase grating mode. The same phenomenon can also be studied in the ferrocholesterics.

3.3.1 Theory

In the present case we consider the magnetization \vec{m} of the grains gradually twisting with the director. We further assume that the medium is locally uniaxial about the local director.

When a plane wavefront of linearly polarized light is incident in a direction normal to the twist axis of the medium, the wavefront will see a variation of refractive index along the twist axis, so that the incident wavefront emerges as a periodically corrugated wavefront with fluctuations in azimuth and ellipticity of the state of the polarization. As the linearly polarized light travels along any layer it splits into two orthogonal elliptic vibrations. The refractive indices of the medium for these two elliptic vibrations are given by [19]

$$\begin{aligned}\frac{1}{n_R^2} &= \frac{1}{2} \left[(\eta_{\perp}(z) + \eta_{\parallel}(z)) - \sqrt{[(\eta_{\perp}(z) - \eta_{\parallel}(z))^2 + 4\gamma^2]} \right] \\ \frac{1}{n_L^2} &= \frac{1}{2} \left[(\eta_{\perp}(z) + \eta_{\parallel}(z)) + \sqrt{[(\eta_{\perp}(z) - \eta_{\parallel}(z))^2 + 4\gamma^2]} \right]\end{aligned}\tag{3.7}$$

where

$$\eta_{\perp}(z) = \frac{\cos^2(\alpha)}{n_1^2} + \frac{\sin^2(\alpha)}{n_2^2} \quad \text{and} \quad \eta_{\parallel}(z) = \frac{1}{n_1^2}$$

Here $\alpha = (2\pi/P)z$, and n_1, n_2 are the refractive indices **along** and **perpendicular** to the local director in the absence of Faraday rotation. The parameter γ is related to the rotatory power p of the medium by the relation

$$\gamma = \frac{\rho\lambda}{\pi(\bar{n})^3} \quad (3.8)$$

Here \bar{n} is the mean refractive index of the medium. These two elliptic vibrations have ellipticity respectively given by

$$\omega_R = \frac{1}{2} \tan^{-1} \left[\frac{2\gamma}{\eta_{\parallel}(z) - \eta_{\perp}(z)} \right] \quad (3.9)$$

$$\omega_L = \pi/2 - \omega_R$$

The elliptic vibration can be mathematically resolved at each point of the emergent wavefront into two linear vibrations polarized along and normal to the twist axis. This results in two periodically corrugated, orthogonal linearly polarized wavefronts given by

$$U_{\parallel}(z) = A_{\parallel}(z) \exp[i\psi_{\parallel}(z)] \quad (3.10)$$

$$U_{\perp}(z) = A_{\perp}(z) \exp[i\psi_{\perp}(z)]$$

where $A_{\parallel}(z)$ and $A_{\perp}(z)$ are the **amplitude** fluctuations and $\psi_{\parallel}(z)$ and $\psi_{\perp}(z)$ are the **phase** fluctuations of these wavefronts, respectively. We assume that the wavelength of the corrugation is large compared to its amplitude so that RN theory can be used to compute the diffraction pattern. The diffraction pattern is obtained by coherently adding the Fourier transform of the two wavefronts.

3.3.2 Results

Using the above theory we have computed the diffraction pattern for experimentally realizable parameters. The diffraction peaks occur for the wavevectors $q = 2\pi(N/P)$. This wavevector is related to the angle of diffraction θ_d through the relation $q = (2\pi/\lambda)\sin(\theta_d)$, N being an integer. The main difference between a ferrocholesteric and a cholesteric is that the optical periodicity in a ferrocholesteric medium is P , the pitch, instead of $P/2$ as in cholesterics. This is due to the magnetization of the grains. This modification of the periodicity gives rise to extra orders (odd orders) of diffraction in addition to the orders (even orders) seen in cholesterics. Also the Faraday rotation results in diffraction for any azimuth φ of the incident linearly polarized light, unlike cholesterics where the diffraction is absent for the linear polarized light incident with azimuth parallel to the twist axis.

Properties of odd orders

We find that for $\varphi = 0$ or $\pi/2$ the odd orders are linearly polarized in the state orthogonal to that of the incident light. For any other general azimuth φ in the range $0 < \varphi < \pi/2$ these orders are in general elliptically polarized. Also the intensity of any odd order is independent of the azimuth of the incident light and only varies with ρ . This is shown in the computed diffraction pattern with intensity as a function of scattering vector in figure 3.1a, 3.1b, 3.2a and 3.2b. Each set gives patterns corresponding to a given value of Faraday rotatory power ρ and for $\varphi = 0, \pi/4$ and $\pi/2$.

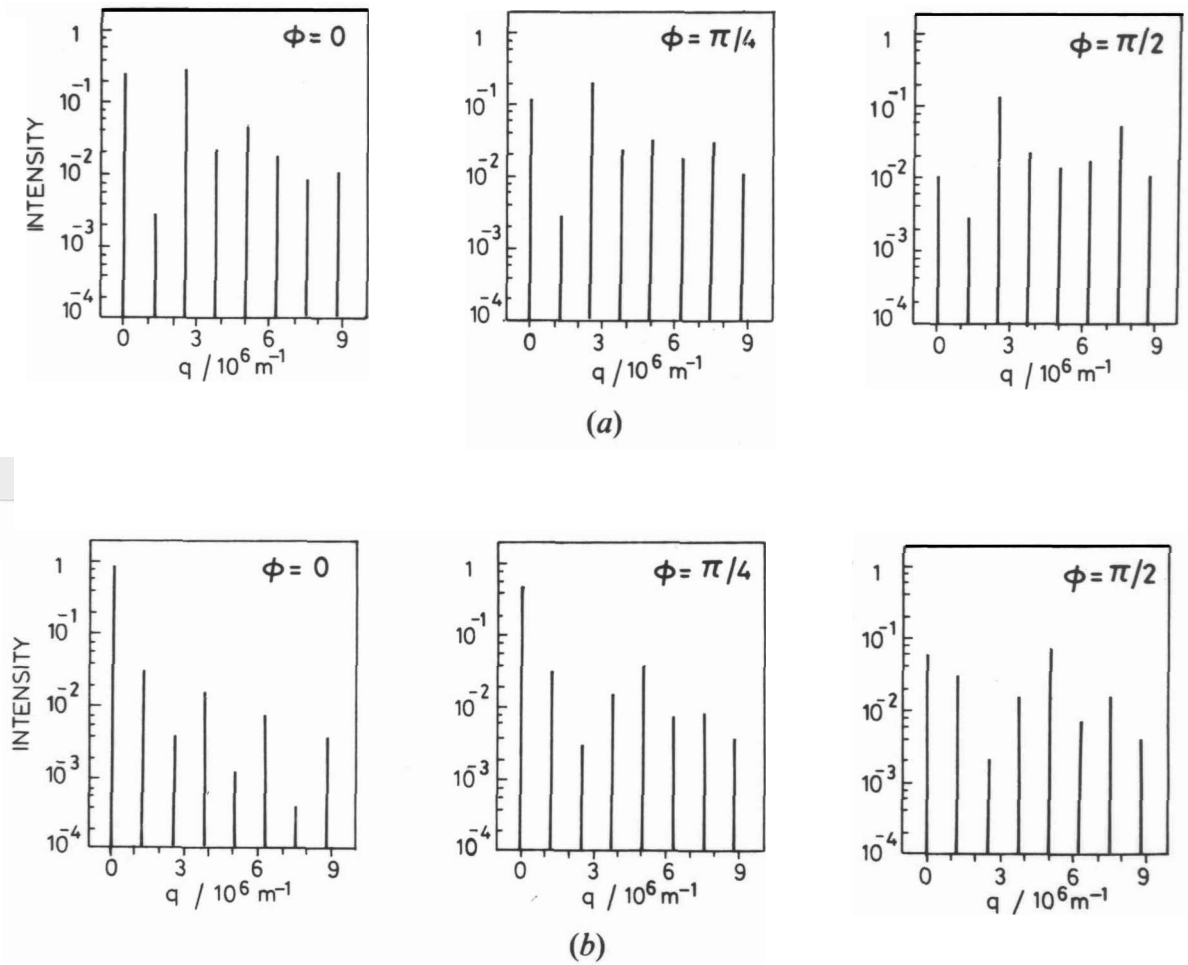


Figure 3.1: Computed diffraction pattern in a ferrocholesteric showing intensity as a function of scattering vector q for $\lambda = 0.633\mu\text{m}$, $A_n = 0.07$, $n_1 = 1.535$, $n_2 = 1.605$, $P = 5\mu\text{m}$ sample thickness ($d = 20\mu\text{m}$). For (a) $\rho_o = 1.92 \times 10^3 \text{rad cm}^{-1}$ and for (b) $\rho_o = 3.54 \times 10^3 \text{rad cm}^{-1}$.

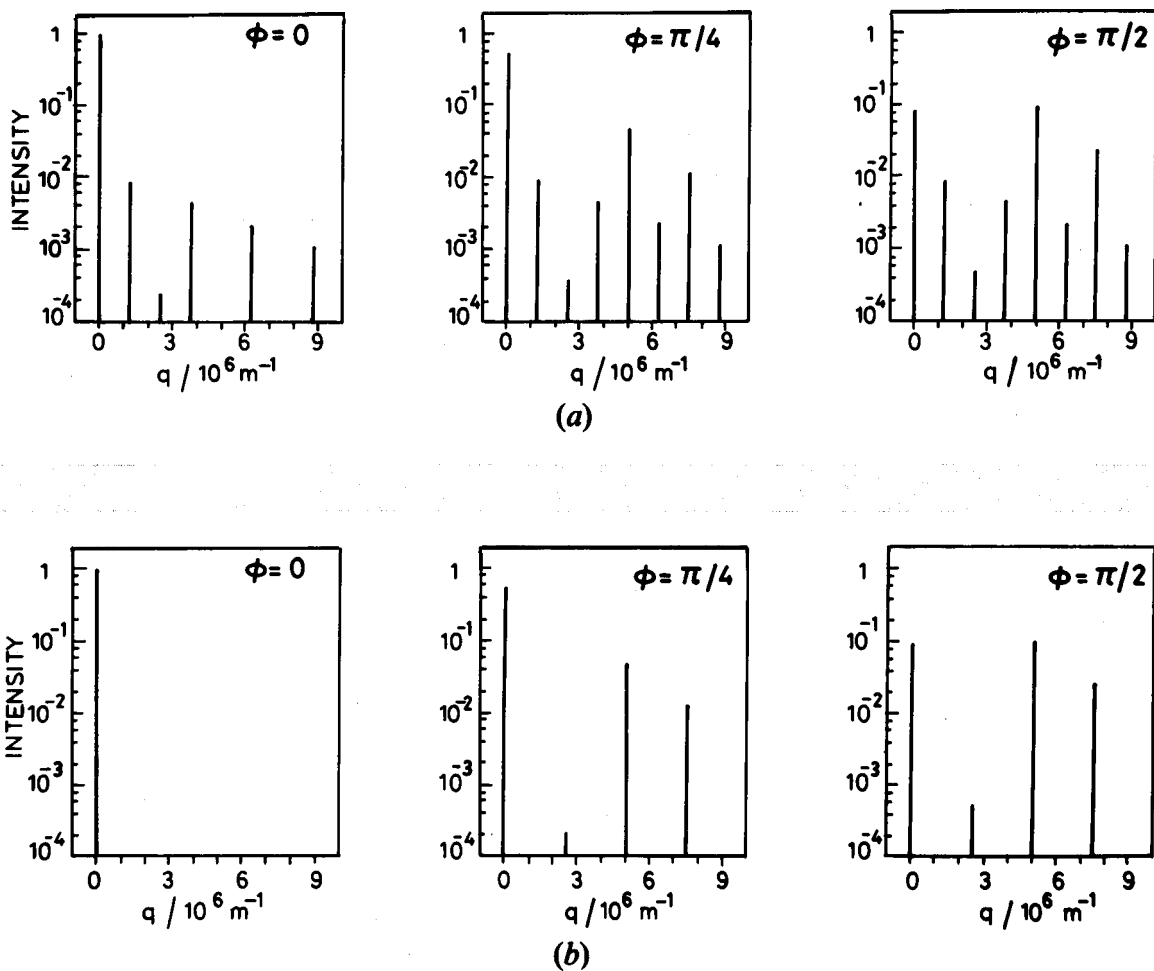


Figure 3.2: Computed diffraction pattern for the same value of Λ , Δn , n_1 , n_2 , P and d For (a) $\rho_o = 1.92 \times 10^2 \text{ rad cm}^{-1}$ and for (b) $\rho_o = 0$ i.e. a normal cholesteric.

Properties of even orders

We find that for $\varphi = 0$ or $\pi/2$ the even orders are linearly polarized in the same state as that of the incident light. For any other general azimuth φ in the range $0 < \varphi < \pi/2$ these orders are also in general elliptically polarized. Faraday rotation not only results in extra orders (the odd orders) but also alters the intensities of these even orders as can be seen from the figures.

All these features are seen even at extremely low values of ρ (see figure 3.2a). It should be noted that in the diffraction patterns calculated for higher values of ρ , the intensity of a higher order grows at the expense of the lower orders (see figure 3.1a). For comparison we give in figure 3.2b the diffraction pattern for zero Faraday rotation i.e. for a normal cholesteric. As is to be expected, in this case the odd orders do not exist. Also for $\varphi = 0$ the entire pattern degenerates to the zeroth order. We would like to remark that in many respects the intensity and the polarization features of diffraction pattern of the odd orders are very similar to those worked out for the Sc* phase [17,20] using RN theory.

In conclusion we have shown here that the inherent Faraday rotation of the transparent magnetic grains remarkably alters the optical properties of ferrocholesterics in both Bragg and the phase grating modes. These optical properties are very different from that of the cholesteric liquid crystals.

References

- [1] P.G. de Gennes and J. Prost, The physics of liquid crystals, 2 edition, Oxford University Press, **1994**.
- [2] J. Rault, P.E. Cladis and J.P. Burger, "*Ferronematics*", Phys. Lett., **32A**, 199 (1970).
- [3] S.H. Chen and N.M. Amer, "Observation of macroscopic collective *behavior* and new texture in magnetically doped liquid crystals", Phys. Rev. Lett. ,**51**, 2298 (1983).
- [4] S.H. Chen and S.H. Chiang, "The magnetic field induced birefringence of the mixture of the *chiral* molecules and the *ferronematic* liquid crystals.", *Mol. Cryst. Liquid Cryst.* , 144, **359** (1987).
- [5] C.F. Hayes, "Magnetic platelets in *a* nematic liquid crystal", *Mol. Cryst. Liquid Cryst.*, 36, **245** (1976).
- [6] P. Fabre, C. Casagrande, M. Veysie, V. Cabuil and R. Massart, "Ferrosmeectics: A new Magnetic and *Mesomorphic* phase", Phys. *Rev. Lett.*, 64, 539 (1990).
- [7] C. Quilliet, V. Ponsinet and V. Cabuil, "Magnetically doped hexagonal *lyotropic* phases", *J. Phys. Chem.*, **98**, 3566 (1994).

- [8] F. Brochard and P.G. de Gennes, "Theory of magnetic suspensions in liquid crystals", *J. Phys.* 31, 691 (1970).
- [9] Y.L. Raïkher, S.V. Burylov and A.N. Zakhlevnykh, "Orientational structure and magnetic properties of a ferronematic in an external field", *Sov. Phys. JETP*, 64, 319 (1986).
- [10] P.B. Sunil Kumar and G.S. Ranganath, "Ferronematics in magnetic and electric fields", *Mol. Cryst. Liquid Cryst.*, 177, 123 (1989).
- [11] S.V. Burylov and Y.L. Raïkher, "Orientation of a solid particle embedded in a monodomain nematic liquid crystal", *Phys. Rev. E*, 50, 358 (1994).
- [12] P.B. Sunil Kumar and G.S. Ranganath, "Structural and optical behavior of cholesteric soliton lattices", *J. Phys. II France*, 3, 1497 (1993).
- [13] Yuvaraj Sah, K.A. Suresh and G.S. Ranganath, "Optical properties of magnetically doped cholesterics", *Liq. Crystals*, 15, 25 (1993).
- [14] R. C. Jones, "A new calculus for the treatment of optical systems I", *J. Opt. Soc. Am.*, 31, 488 (1941).
- [15] S. Chandrasekhar, *Liquid crystals*, 2 edition, Cambridge University Press, 1992.
- [16] R. C. Jones, "A new calculus for the treatment of optical systems VII. Properties of N-matrix", *J. Opt. Soc. Am.*, 38, 671 (1948).
- [17] K.A. Suresh, P.B. Sunil Kumar and G.S. Ranganath, "Optical diffraction in twisted liquid-crystalline media - phase grating mode", *Liq. Crystals*, 11, 73 (1992).

- [18] E. Sackmann, S. Meiboom, L.C. Snyder, A.E. Meimner and R. E. Dietz, "On the structure of the liquid crystalline state of cholesterol derivative ", *J. Am. Chem. Soc.*, **90**, 3567 (1968).
- [19] G. N. Ramachandran and S. Ramaseshan, *Handbuch der physik*, Vol 25, part 1, (Springer Verlag), Page 81 (1961).
- [20] R. V. Johnson and A. R. Tanguay, "Optical beam propagation method for birefringent phase grating diffraction ", *Optical Engineering*, 25, 235 (1986).

Chapter 4

Optical diffraction in chiral smectic C liquid crystals : Experimental study

4.1 Introduction

In the previous chapters we discussed some interesting optical properties associated with cholesterics and ferrocholesterics. In this chapter we investigate another structurally interesting twisted liquid crystalline phase, namely, chiral smectic C (Sc^*).

The Sc^* phase has a helical stack of layers of uniformly tilted molecules. Using the symmetry arguments Meyer proposed that this (Sc^*) phase will be ferroelectric. Subsequently Meyer et.al. [1] synthesized an appropriate Sc^* system and showed that this phase is indeed a ferroelectric liquid crystalline phase. After the discovery of ferroelectricity in the Sc^* phase it has been a subject of various physical studies [2,3,4]. Technologically, it became very important after Clark and Lagerwall [5] demonstrated the submicrosecond response of the director to the applied electric field that can be exploited in fast switching liquid crystal display devices. Another consequence of the chirality of the molecules is the twisted structure of the phase which gives rise to some very interesting optical properties.

There have been many studies on the light propagation in Sc^* in the Bragg mode [6,7,8]. At normal incidence Sc^* phase shows optical properties similar to that

shown by the cholesteric phase. At oblique incidence Sc^* also exhibits higher order reflections but polarization features of these reflection bands are very different from that found in the cholesteric reflection bands. Berreman [6] showed, for Sc^* , that in the Bragg band corresponding to the full pitch, the reflected light is orthogonally polarized with respect to the incident light. Further, Oldano [7,8] predicted that the polarization of the reflected light is not a smooth function of the tilt angle of the Sc^* phase. He showed that there exists a critical tilt angle above which there is a reversal in the polarization features of the Bragg band.

Studies in the phase grating mode (propagation of light perpendicular to the twist axis) have drawn very little attention in literature. In this mode the Sc^* medium acts as a one dimensional phase grating for the incident light resulting in the optical diffraction. The RN theory of phase gratings was generalized and used by Suresh et.al. [9] to compute the diffraction pattern for Sc^* . They predicted that the odd orders of diffraction have very different intensity and polarization features as compared to the even orders of diffraction. For example, one finds that for incident linearly polarized light, at a general azimuth φ , the odd orders are linearly polarized. The intensities in these orders are independent of φ . In contrast, the even orders are, in general, elliptically polarized with their intensity depending on φ . Also for incident wave polarized parallel or perpendicular to the twist axis the odd orders are always polarized in the orthogonal linear state while the even orders are polarized in the same linear state with respect to incident vibration. In view of these interesting intensity and polarization predictions, we undertook an experimental study of the diffraction in Sc^* [10]. In this chapter we present the unusual intensity and polarization features of the diffraction pattern associated with Sc^* in phase

grating mode.

4.2 Description of the Experiment

4.2.1 Material used

The experiments were carried out on the commercially obtained sample BDH SCEG. We chose this sample since it is a Sc* at room temperature. It has the sequence of transitions



The pitch of the sample in the Sc* phase is temperature dependent and at room temperature it was about 5 μm and was suitable for getting enough diffraction orders on the screen. One convenient and accurate method to evaluate the pitch is by measuring the angular separation of the first order diffraction from the direct beam. The temperature variation of the pitch in the Sc* phase of this compound is shown in figure 4.1. The tilt angle for this material in the Sc* phase varies from 17° to 23° over the temperature from 60°C to 40°C. The birefringence of the medium at room temperature is 0.18.

4.2.2 Sample preparation

To get monodomain samples suitable for phase grating geometry we employed the following procedure: sample cells were prepared using glass plates which were previously treated with polyimide and rubbed in the parallel direction. Cells of different thicknesses were obtained using mylar spacers of thicknesses 23,50,125 and 250 μm .

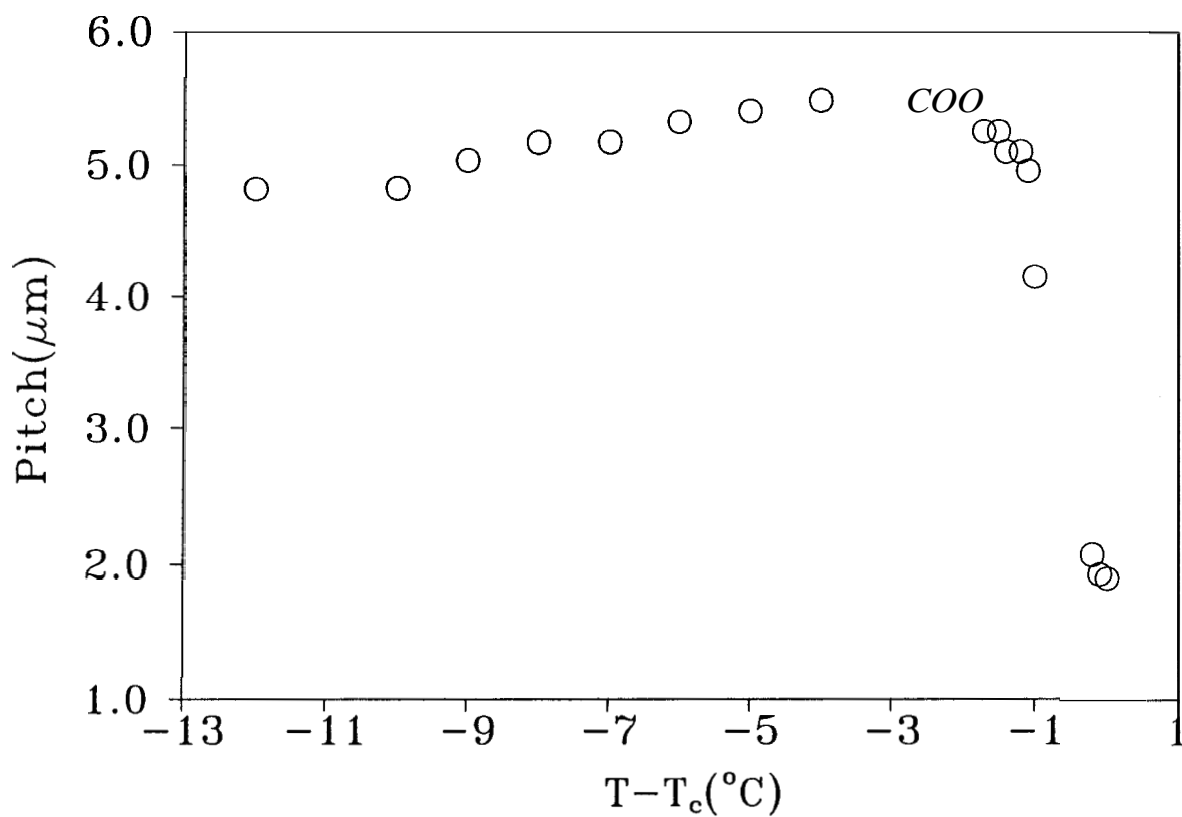


Figure 4.1: The pitch of the sample SCE6 as a function of temperature. Here T_c represents smectic A - Sc* transition temperature. The pitch is evaluated by measuring the angular separation of the first order diffraction with the direct beam. A $50\mu\text{m}$ cell was used for the measurement.

Later, the cells were filled with the sample in the isotropic phase and cooled very slowly across the cholesteric to smectic A (S_A) phase transition in the presence of a magnetic field of strength 2.4 Tesla applied parallel to the rubbing direction. Observations under a Leitz polarizing microscope revealed the formation of very good homogeneous monodomain S_A phase which on further cooling resulted in Sc^* with very uniform parallel striations [11,12]. These striations arise due to the uniform twisted structure of the phase and were perpendicular to the rubbed direction (twist axis). The photograph of a 50 μ m aligned sample is shown in figure 4.2. For samples of thicknesses lower than 23 μ m, due to the surface effects, the helical structure got considerably distorted and hence were not used.

4.2.3 Experimental setup

The schematic diagram of the experimental setup is shown in figure 4.3. The aligned cell was placed inside a locally fabricated heater mounted on the center table of a goniometer. The temperature of the sample was measured with a K type thermocouple with an accuracy of $\pm 0.1^\circ\text{C}$. A polarized 2 mW He-Ne laser ($\lambda=632.8 \text{ nm}$) was mounted on the fixed arm of the goniometer. A halfwave plate was used to select the desired state of incident polarization. The light was allowed to fall normally on the sample. The diffracted light was passed through an analyzer and was subsequently collected on a photodiode (Centronic OSD-5) fitted on the moving arm of the goniometer. The output signal of the photodiode was measured with a Keithley 181 nanovoltmeter (NVM) and was also fed into a Graphtec servocorder.

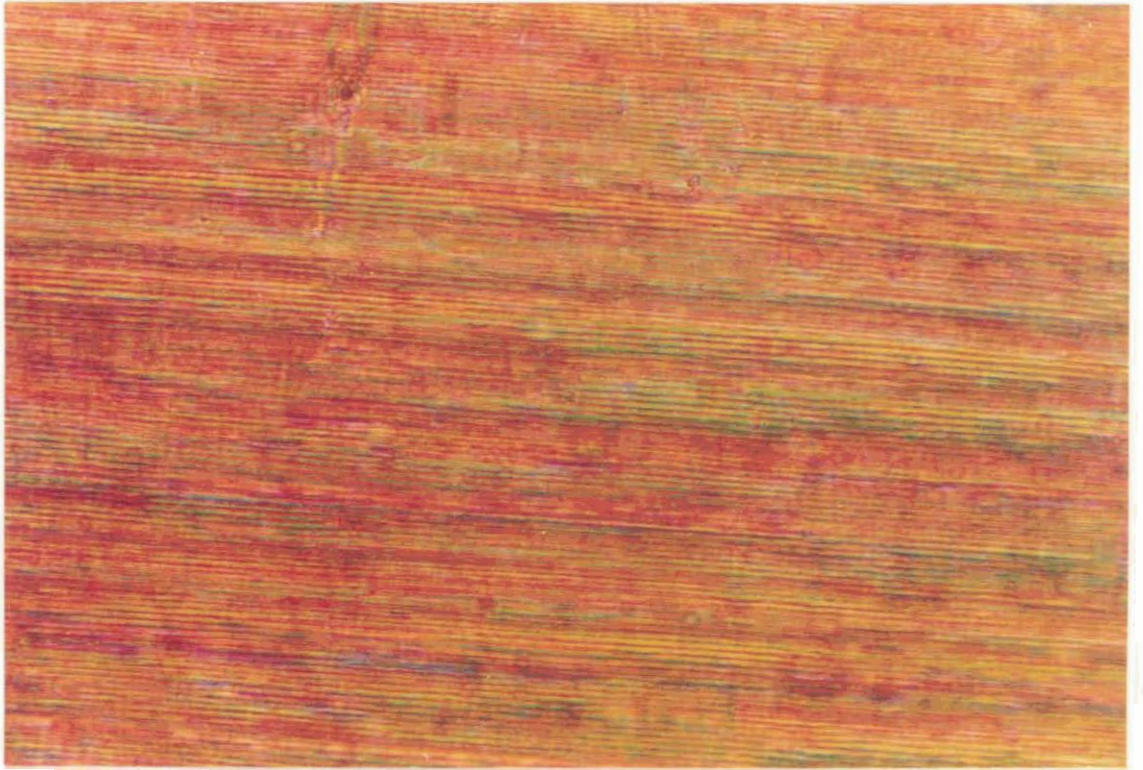


Figure 4.2: The uniform parallel striations in the aligned Sc* phase of SCE6 observed under a polarizing microscope. (Sample thickness $50\mu\text{m}$).

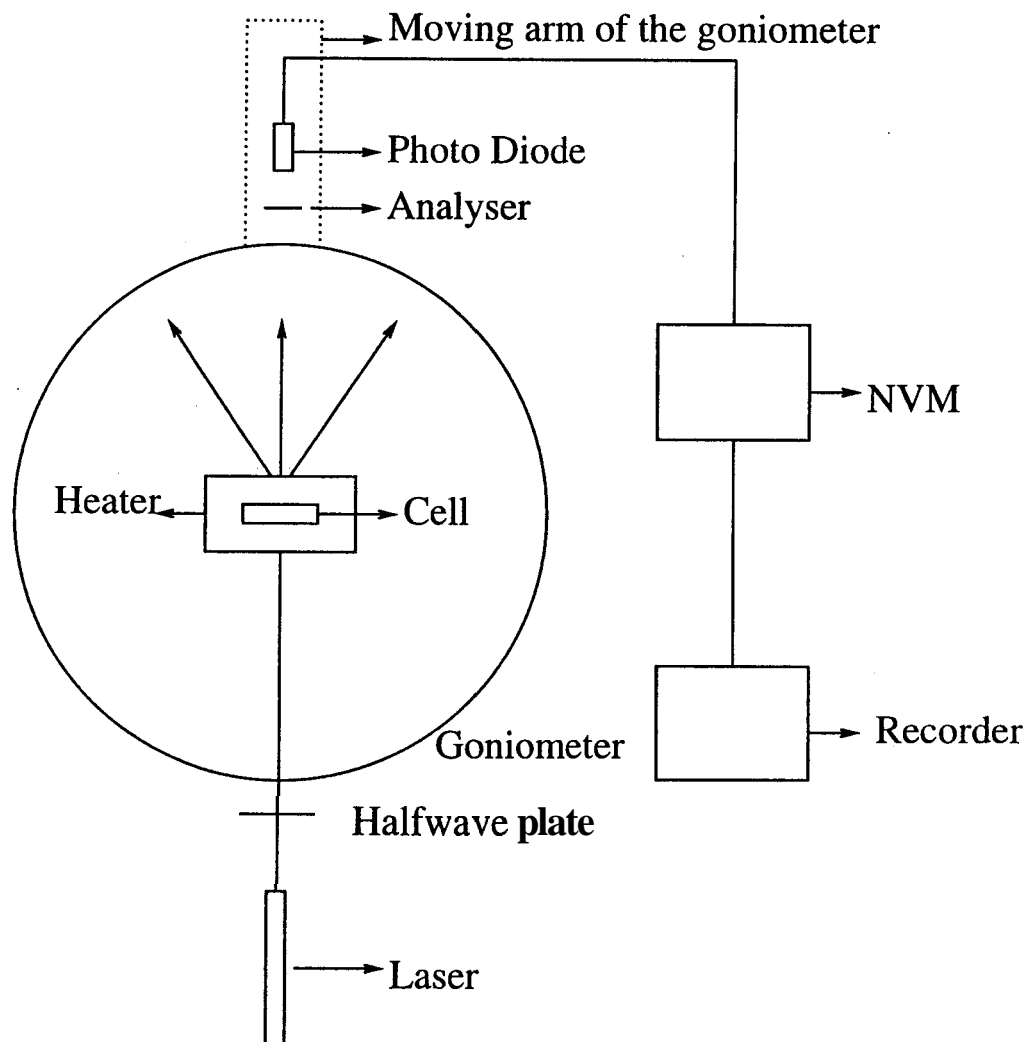


Figure 4.3: The schematic diagram of the experimental setup used for the diffraction experiment.

4.3 Results and discussion

In our experiments, for incident linearly polarized light we got sharp diffraction orders. Typically we got 6 orders on either side of the direct beam. Figure 4.4 shows the diffraction patterns of a $50\ \mu\text{m}$ sample for the geometries HH, HV, VH and VV (H denotes polarization parallel to the twist axis and V denotes polarization perpendicular to the twist axis. The first letter indicates the state of polarization of the incident light and the second letter indicates the polarization state in which the diffracted beam is analyzed).

We show in figure 4.5(a), 4.5(b) and 4.6 the measured diffracted intensity in the various orders for $23\ \mu\text{m}$, $50\ \mu\text{m}$ and $125\ \mu\text{m}$ sample thicknesses. Surprisingly, the obtained results contradict to the predictions of the generalized RN theory. As one can note from the figures 4.5(a), 4.5(b) and 4.6 that the intensity in the **HH geometry** (open circles) is always very much higher than the intensity in the **HV** (closed circles) geometry for all orders. Also the intensity in the **VH geometry** (open squares) is always higher than the intensity in the **VV geometry** (closed squares). That is, in all the orders, the diffracted light is nearly linearly polarized parallel to the twist axis. Interestingly, this behaviour is observed in samples of thickness $23\ \mu\text{m}$ and $50\ \mu\text{m}$ at all temperatures. For the $125\ \mu\text{m}$ also the same behaviour was found at all temperatures except near the $\text{Sc}^* - \text{S}_A$ transition temperature. We can also note that in this sample ($125\ \mu\text{m}$) the intensity of the first order diffraction for the **HH** and **VH** geometries is less than that of the second order (see figure 4.6). This phenomenon is known as the wandering of intensity between various orders. This is a common feature of diffraction in the phase grating mode that makes it different

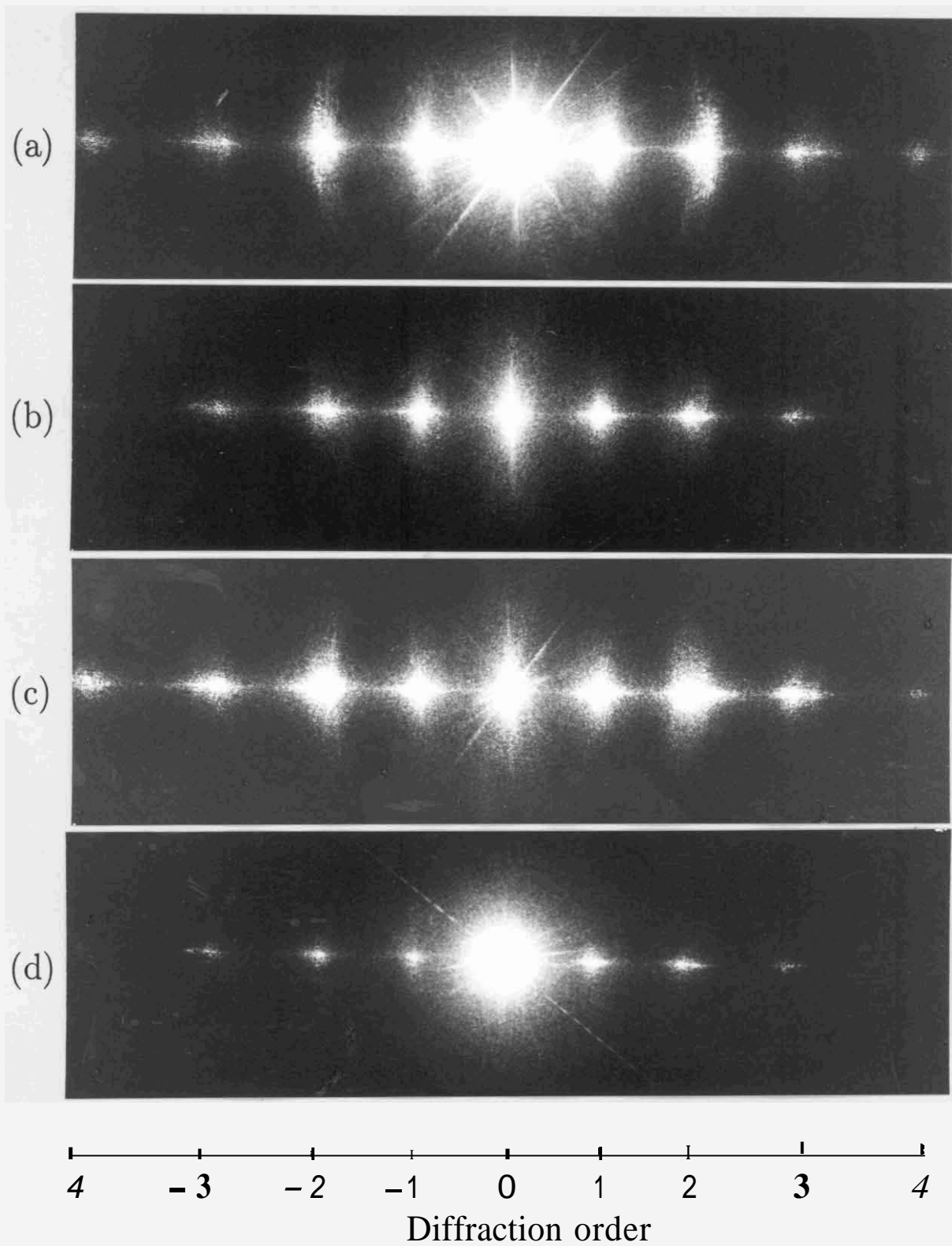


Figure 4.4: The photographs of the diffraction patterns of a $50\mu\text{m}$ sample in (a) HH (b) HV (c) VH and (d) VV geometries.

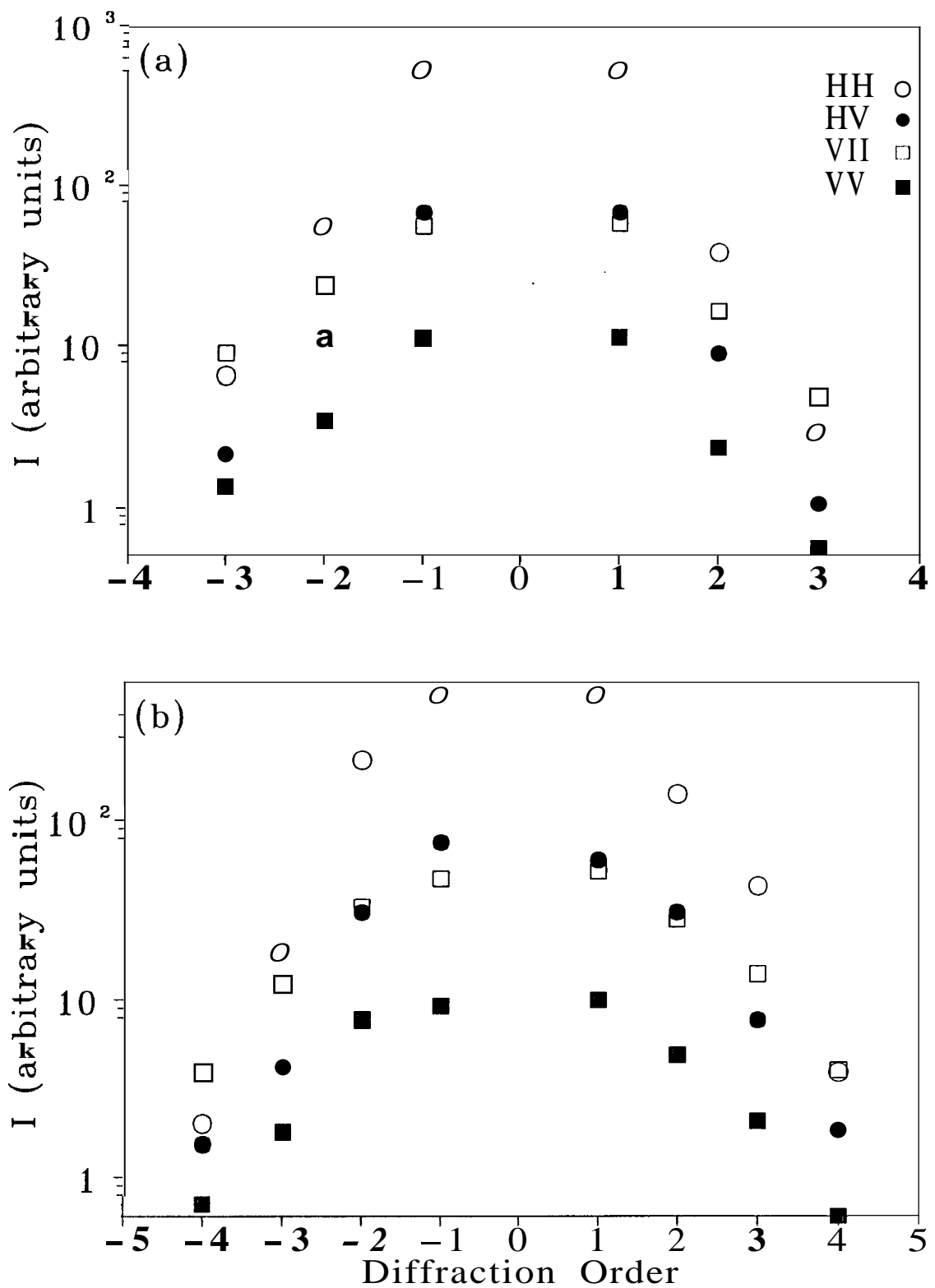


Figure 4.5: The intensity I (arbitrary units) in the diffraction orders shown for various geometries for samples of thickness (a) $23\mu\text{m}$, (b) $50\mu\text{m}$ at temperature = 50.6°C . Here one may notice that in every order $I(\text{HH}) > I(\text{HV})$ and $I(\text{VII}) > I(\text{VV})$. The intensity of the direct beam is too high to be shown here. The asymmetry in the intensity pattern for some orders is due to slight imperfections in the orientation of the sample.

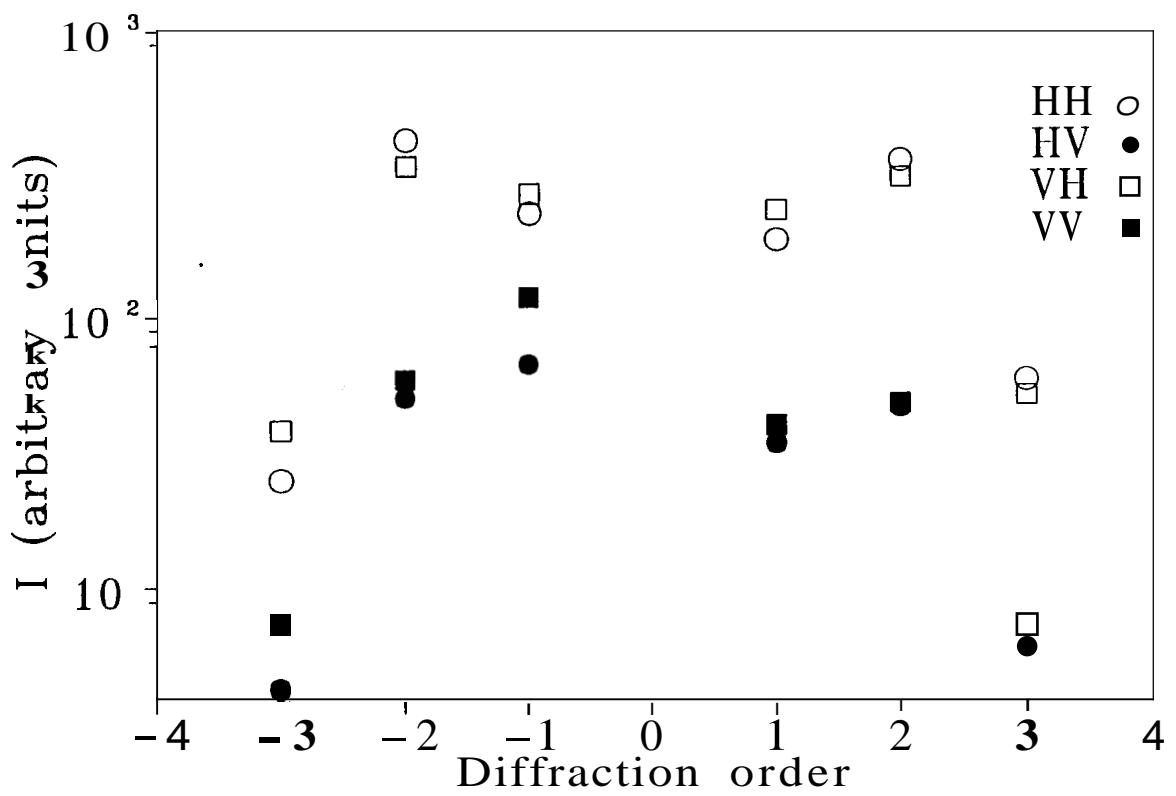


Figure 4.6: The intensity I (arbitrary units) in the diffraction orders shown for various geometries. (sample thickness $125 \mu\text{m}$, temperature = 45.5°C).

from the amplitude gratings where there is a monotonic decrease in intensity with increase in order.

However, in a sample with a thickness of $250 \mu\text{m}$, we find a more interesting behaviour. At low temperatures ($\leq 46^\circ\text{C}$) the intensity and polarization features are the same as that for the thin samples, i.e, the diffracted intensity is more for the HH and VH geometries than that in the HV and VV geometries respectively. But at higher temperatures ($\geq 50.6^\circ\text{C}$), the behaviour gets completely reversed. This is shown in figure 4.7(a) and 4.7(b) respectively. At high temperatures the intensity of the diffracted light in the VV geometry becomes more intense than the intensity in the VH geometry. Even the intensity in the HV geometry is more than that in HH geometry. Hence in this case, in all the orders, the component of the diffracted light perpendicular to the twist axis is more than the component parallel to the twist axis. Thus in this particular sample, one can drastically change the polarization features of the diffraction orders by varying the temperature of the sample.

We would like to remark that in all these geometries, in all the cells, the zeroth order is in a polarization state close to that of the incident polarization. i.e. it has a small orthogonal component.

These results are certainly not in agreement with the generalized RN theory. We know that the theory assumes that in the corrugated wavefront, the amplitude of the phase modulation is much less than the wavelength of the phase modulation. In effect it assumes that there is no appreciable diffraction taking place inside the medium and the incident wavefront gets considerably corrugated only after emerging out of the sample. This assumption is valid only for low birefringence and small

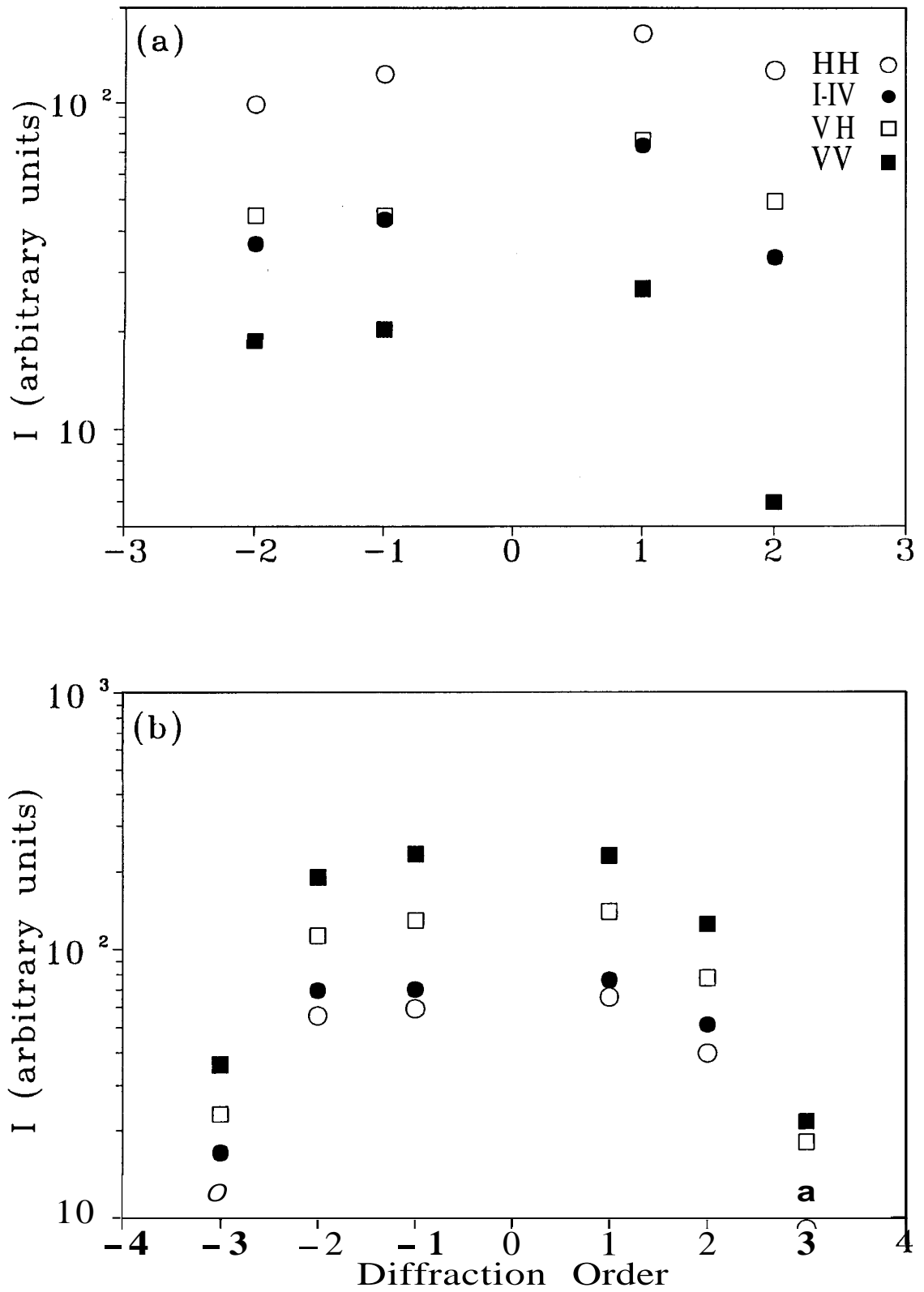


Figure 4.7: The intensity I (arbitrary units) in the diffraction orders shown for various geometries for a $250\mu\text{m}$ sample at (a) 45.5°C and at (b) 50.6°C .

sample thicknesses. However, in the present case, the material has a high birefringence and the used sample thicknesses are large. Therefore in this case RN theory is not valid. We have to use a more rigorous theory for anisotropic dielectric gratings which incorporates the internal diffractions inside the medium and takes care of the boundary effects. In the next chapter we give a more general theory based on Rokushima and Yamakita's approach [13] to account for these experimental results that are very surprising and interesting.

References

- [1] R.B. Meyer, L. Liebert, L. Strzelecki and P. Keller, "Ferroelectric liquid crystals", *J. de Phys*, 36, L-69 (1975).
- [2] L.J. Yu, H. Lee, C.S. Bak and M.M. Labes, " Observation of pyroelectricity in chiral smectic *C* and Hexatic liquid crystal" , *Phys. Rev. Lett.*, 36, 388 (1976).
- [3] P. Pieranski, E. Guyon and P. Keller, "Shear flow induced polarization in *ferroelectric smectic C*", *J. Phys.*,**36**, 1005 (1975).
- [4] S. Garoff and R.B. Meyer, "Electroclinic effect at the A-C phase change in chiral Smectic liquid crystal", *Phys. Rev. Lett.*, 38, 848 (1976).
- [5] N.A. Clark and S.T. Lagerwall, " Submicrosecond bistable electro-optic switching in liquid crystals " , *Appl. Phys. Lett.*, 36, 899 (1980).
- [6] D. W. Berreman, "Twisted *smectic C* phase: *unique* optical properties", *Mol. Cryst. Liquid Cryst.*, 22, 175 (1973).
- [7] C. Oldano, "Existence of a critical tilt angle for the optical properties of *chiral* smectic liquid crystal" , *Phy. Rev. Lett.*, 53, 2413 (1984).

- [8] C. Oldano, I. Allia and L. Trossi, "Optical properties of *anisotropic* periodic helical structures", *J. Physics*, 46, 573 (1985).
- [9] K.A. Suresh, P.B. Sunil Kumar and G.S. Ranganath, "Optical diffraction in twisted liquid-crystalline media - phase grating mode", *Liq. Crystals*, 11, 73 (1992).
- [10] K.A. Suresh, Yuvaraj Sah, P.B. Sunil Kumar and G.S. Ranganath, "Optical diffraction in chiral smectic *C* liquid crystal", *Phys. Rev. Lett.*, 72, 2863 (1994).
- [11] I. M. Lagarde, "Observation of ferroelectrical monodomains in the *chiral smectic C* liquid crystals", *J. de Phys.*, 37, C-129 (1976).
- [12] K. Kondo, F. Kobayashi, H. Takezoe, A. Fukuda and E. Kuze, "Temperature variation of helical pitch in chiral smectic *C* liquid crystals as observed with an optical microscope", *Jpn. J. Appl. Phys.*, 19, 2293 (1980).
- [13] K. Rokushima and J. Yamakita, "Analysis of anisotropic dielectric gratings", *J. Opt. Soc. Ame.*, 73, 901 (1983).